Epilepsy Research (2015) 110, 95—104

journal homepage: www.elsevier.com/locate/epilepsyres

Diffusion tensor imaging tractography of Meyer's loop in planning resective surgery for drug-resistant temporal lobe epilepsy

Jija S. James[b], Ashalatha Radhakrishnan[a,*], Bejoy Thomas[b], Mini Madhusoodanan[a], Chandrashekharan Kesavadas[b], Mathew Abraham[a], Ramshekhar Menon[a], Chaturbhuj Rathore[a], George Vilanilam[a]

[a] *R Madhavan Nayar Centre for Comprehensive Epilepsy Care, Sree Chitra Tirunal Institute for Medical Sciences and Technology, Trivandrum 695011, India*
[b] *Department of Imaging and Interventional Radiology, Sree Chitra Tirunal Institute for Medical Sciences and Technology, Trivandrum 695011, India*

Received 13 August 2014; received in revised form 9 November 2014; accepted 19 November 2014
Available online 27 November 2014

KEYWORDS
Meyer's loop;
Visual field defect;
DTIT;
Temporal lobe epilepsy;
Optic radiation;
Anterior temporal lobectomy

Summary
Purpose: Whether Meyer's loop (ML) tracking using diffusion tensor imaging tractography (DTIT) can be utilized to avoid post-operative visual field deficits (VFD) after anterior temporal lobectomy (ATL) for drug-resistant temporal lobe epilepsy (TLE) using a large cohort of controls and patients. Also, we wanted to create a normative atlas of ML in normal population.
Methods: DTIT was used to study ML in 75 healthy subjects and 25 patients with and without VFD following ATL. 1.5 T MRI echo-planar DTI sequences with DTI data were processed in Nordic ICE using a probabilistic method; a multiple region of interest technique was used for reconstruction of optic radiation trajectory. Visual fields were assessed in patients pre- and post-operatively.
Results: Results of ANOVA showed that the left ML-TP distance was less than right across all groups ($p = 0.01$). The average distance of ML from left temporal pole was 37.44 ± 4.7 mm (range: 32.2—46.6 mm) and from right temporal pole 39.08 ± 4.9 mm (range: 34.3—49.7 mm). Average distance of left and right temporal pole to tip of temporal horn was 28.32 ± 2.03 mm (range: 26.4—32.8 mm) and was 28.92 ± 2.09 mm, respectively (range: 25.9—33.3 mm). If the anterior limit of the Meyer's loop was $\leq$38 mm on the right and $\leq$35 mm on the left from the temporal pole, they are at a greater risk of developing VFDs.

* Corresponding author. Tel.: +91 471 2524282; fax: +91 471 2446433.
E-mail address: drashalatha@sctimst.ac.in (A. Radhakrishnan).

http://dx.doi.org/10.1016/j.eplepsyres.2014.11.020

Conclusions: DTIT is a novel technique to delineate ML and plays an important role in planning surgical resection in TLE to predict post-operative visual performance and disability.

Introduction

Anterior temporal lobectomy (ATL) is a widely accepted surgery for temporal lobe epilepsy (TLE). However, a standard ATL can sometimes cause optic radiation (Meyer's loop, ML) injury in the temporal lobe, which may lead to an incongruous superior quadrantanopia of varying severity. Although the degree of visual field defect (VFD) greatly depends on the anatomic range of the resection, it is well known that the same extent of resection can result in different degrees of VFD in different individuals. The reported rates of VFDs after ATL range from 60 to 100% in various studies (Jensen and Seedorff, 1976; Barton et al., 2005). This is especially important in the context of pre-surgical counseling of patients who undergo ATL for drug-resistant TLE, both lesional and non-lesional, where the field defect that can happen after surgery needs to be detailed to the patient and the family.

The optic radiation (OR) shows high degree of intersubject variability and cannot be delineated on conventional magnetic resonance imaging (MRI) since the variability of white matter signals are minimal. The anterior limit of ML has been estimated to be anywhere from 20 to 60 mm posterior of the temporal pole, with much lower estimates in more recent studies (Salmon et al., 2000; Nilsson et al., 2004; Yogarajah et al., 2009). Although cadaveric study still remains the gold standard to delineate the optic radiations and ML, diffusion tensor imaging tractography (DTIT) with an individual 3D brain model provides a complementary method to study the OR and ML in vivo. DTIT is a non-invasive advanced neuroimaging technique that allows the delineation of microstructural architecture of white matter fiber pathways in vivo which has been standardized in our center (Radhakrishnan et al., 2011). This technique can probe the magnitude of diffusion of water molecules in different directions in each voxel (Basser, 1995; Mori and Van, 2002). The location of the ML is variable with its anterior position varying as much as 1—2 cm between individuals (Ebeling and Reulen, 1988). So it is important to identify the varying patterns of OR in different individuals and in different populations to study their inter individual variability.

To minimize the occurrence of VFD after ATL, a surgeon may have to limit his resection to standard measurements especially in individuals where their occupation or driving is likely to be jeopardized. But this method of limiting the resection to avoid VFD may not help all patients, since the anatomy is variable in each individual and in different populations, thus causing this over simplification irrational and patient can sometimes become a ''triple loser'' by not becoming seizure-free despite financial losses he/she incurs paying for surgery, at the same time ending up with a VFD. Hence, a procedure like DTIT of ML if standardized and utilized routinely may play an important role in the presurgical evaluation of anterior temporal lobe resections in TLE to avoid postsurgical VFD.

The aim of the present study was to create a normative atlas of Meyer's loop for clinical and research purposes on a large age-matched population of male and female participants which has not hitherto been established. The objectives while doing so were to

(1) Map the extent of optic radiation and especially the ML in a sizeable cohort of healthy normal adults.
(2) To assess the interindividual variability in the extent of the ML in normal healthy volunteers at various anatomic locations.
(3) To measure the fractional anisotropy (FA) indices, mean diffusivity (MD) values and fiber tract volume of ML using diffusion tensor imaging and fiber tractographic techniques.
(4) Application of these measurements to decide on the safe limit of anterior temporal lobe resection in refractory TLE on either side (right and left) not causing VFD in patients.

Materials and methods

Subjects

The study was undertaken at the R. Madhavan Nayar Center for Comprehensive Epilepsy Care and Department of Imaging and Interventional Radiology, Sree Chitra Tirunal Institute for Medical Sciences and Technology, Trivandrum, Kerala, South India, a tertiary referral center with ample expertise in tackling difficult-to-treat epilepsies. Data were obtained from 75 healthy age matched subjects (age range: 22—37 years, 45 males and 30 females; all right handed) with no head injury, history of prior neurosurgery, visual deficits or psychiatric illnesses. The controls were chosen from patients who underwent brain MRI for one of the following indications: chronic headache, trigeminal neuralgia, transient ischemic attack, optic neuritis and acute meningitis; but the brain parenchyma and the optic radiations were essentially normal. Also, it was undertaken in 25 consecutive patients, all right handed, with and without VFD after a standard ATL for refractory TLE of various etiologies (mesial temporal sclerosis-9, tumors-12, cavernoma-2, gliosis-2). Two neurosurgeons (MA and GV) experienced in performing epilepsy surgeries conducts a standard ATL in our center, a maximum of 6—6.5 cm of the non-dominant temporal lobe and 4.5—5 cm of the dominant temporal lobe are resected. The mesial resection includes the amygdala and approximately 3—4 cm of the hippocampus.

The Institutional Ethics committee approved the study and a written informed consent was obtained from all subjects (normal subjects and patients) after explaining the procedure and the utility of the study. All the participants co-operated with the study procedure. All patients were

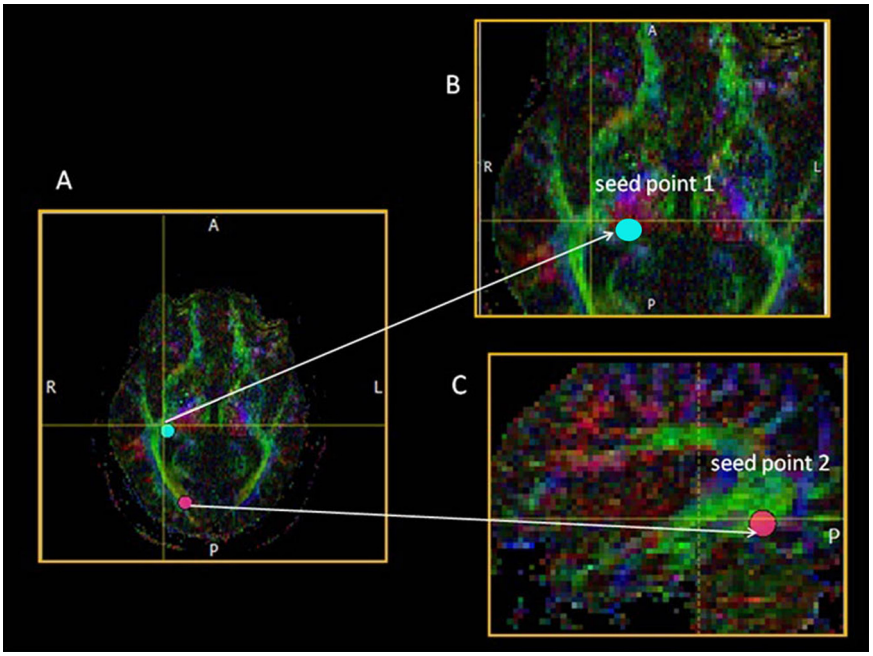

Fig. 1 (A) Probabilistic tractography of Meyer's loop using the seed/target approach or exhaustive search. Optic radiation pathway in color coded FA map, where fibers running in anterior—posterior direction appears green in color. (B) A multiple region of interest (ROI) technique used for reconstruction of optic radiation trajectory. The first seed region was identified and the ROI was drawn on lateral geniculate nucleus on axial slice. (C) For the second seed region, the calcarine fissure was identified and second ROI was drawn on a sagittal slice and then tracking the fiber tracts connecting the two seed points using the AND operator. (For interpretation of the references to color in this figure legend, the reader is referred to the web version of this article.)

examined using diffusion tensor MR imaging to track the OR and ML and automated perimetry to chart their visual fields before and 3 months after surgery.

MRI acquisition

MRI studies were performed on a 1.5 T MRI (Avanto SQ Engine, Siemens, Erlangen, Germany). Anatomic landmark images of the entire head were obtained with a 3-D spoiled gradient-recalled acquisition in the steady state sequence (3-D FLASH; TR/TE 11/4.94 ms, flip angle 15°, FOV 256 mm, slice thickness 1 mm, matrix 256 × 256), following the availability of 3-D FLAIR (TR/TE/TI 5000/405/1800 ms, FOV 256 mm, slice thickness 1 mm, matrix 256 × 256) in order to co-register the tractography data for better visualization. A spin-echo, echo-planar DTI sequence was performed with diffusion gradients along 30 non-collinear directions with the following imaging parameters: TR 9900 ms, TE 102 ms, matrix 112 × 96, field of view 220 mm^2, 2 mm slice thickness with 1.5 mm gap averaged twice and with a *b* factor of 0 and 1400 s/mm^2.

Diffusion tensor imaging tractography (DTIT)

All DTI data were imported to a dedicated software called Myrian XT-Brain (Intrasense-Modi Medicare) which works on a windows based workstation. The DTI module of Nordic ICE generates various parametric maps; color-coded DTI, FA, RA (radial anisotropy), ADC (apparent diffusion coefficient), Trace W and tensor Eigen values. It also provides integrated correction scheme for motion and eddy current artifacts. The probabilistic tractography of ML was done using the seed/target approach. We optimized the tracking results by selection of termination criteria, FA-threshold = 0.2 and tract turning angle = 30°. First we identified the optic radiation pathway in color coded FA map, where fibers running in anterior—posterior direction appears green in color (Fig. 1A—C).

A multiple region of interest (ROI) technique was used for reconstruction of optic radiation trajectory. Reproducibility of fiber pathway reconstruction is possible by saving the ROI radius and location. We used the logical operator, ''AND'' for tract reconstruction. Choice of operations depended on the characteristic trajectory of the tract. The first seed region was identified and the ROI was drawn on LGN on an axial slice and fibers penetrating these regions were identified. For the second seed region, the calcarine fissure was identified and second ROI was drawn on a sagittal slice which lies close to the midline and then tracking the fiber tracts connecting the two seed points using the AND operator. For 3-D visualization of white matter bundles, we superimposed the tractography data on to ADC map (Fig. 2A and B) image. We also calculated tract specific statistics (tract volume, length, FA and MD values) for both right and left Meyer's loop of all subjects. For each patient the quality of the tractography was validated by looking at the results which should simulate the optic radiations and all three components of the optic radiations should be visualized clearly.

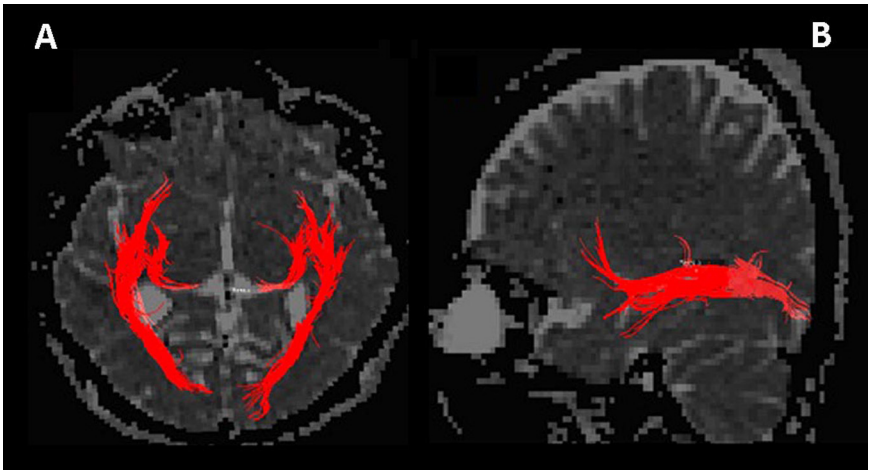

Fig. 2 (A) 3-D visualization of white matter bundles by superimposing the tractography data on to ADC map image in axial and (B) sagittal slices respectively.

Visual field charting

Pre- and post-surgery visual field charting was done using an automated perimeter, Mon CV1Visual Field Analyzer (Metro vision, 4 rue des Platanes 59840 PERENCHIES, France). It provides an ambient luminance of 10 cd/m^2 (low photopic level that reduces the time for light adaptation), standardized test sizes (size II = test seen under a visual angle of 13 arc min, III = 26 min, IV = 53 min, V = 103 min), a white color, calibrated luminance levels and a constant presentation time of 300 ms. The maps of measured values displays values of each point measured in the visual field and the maps of density levels facilitates the interpretation of the location and shape of the deficits. Thus the vision monitor combines a unique representation of the advantages of the different representation modes viz. measured values, map of density levels and isopters. The charting was done pre-operatively and at 3 month follow-up visit after surgery because in the immediate post-operative period, the VF charting can give erroneous results due to the adjoining edema and blood or CSF collection in the operated site.

Data analysis

Further data analysis was also carried out in Myrian XT-Brain (Intrasense-Modi Medicare). For better visualization of fiber tracts, we superimposed the tractographic data into a high resolution T1 weighted image (3-D fluid attenuated inversion recovery sequence (3D-FLAIR). From the superimposed data, we identified mainly three anatomical landmarks; anterior tip of the Meyer's loop, anterior tip of the temporal horn and anterior tip of the temporal pole. These landmarks are used to measure three distances: (a) distance from the temporal pole to the anterior limit of Meyers loop (TP-ML), (b) distance from the temporal pole to the tip of the temporal horn (TP-TH) and (c) distance from temporal horn to anterior limit of Meyers loop (TH-ML). TH-ML distance was obtained by subtracting TP-TH from TP-ML distance. FA and MD values for both right and left Meyer's loop was computed using mirror ROI analysis approach provided by Nordic ICE's diffusion evaluation module.

This was done in both the normal healthy controls and in patients pre- and post-surgically. The seed and target areas for the presurgical tractographies were recorded, with identical seed and target areas used for postsurgical images. To note the most anterior point of the Meyer's loop in the images, tractography of the uncinate fasciculus (which is located just anterior to the most anterior point of the Meyer's loop) was also delineated (Taoka et al., 2008). The seed area in the white matter of the frontal lobe was located in the coronal plane at the tip of the frontal horn of the lateral ventricle, and the target area in white matter was located in the coronal plane at the tip of the inferior horn of the lateral ventricle in the ipsilateral temporal tip (Taoka et al., 2005). We measured the distance between the anterior limit of the Meyer's loop and the posterior limit of the uncinate fasciculus and thus ascertained the accuracy of the tractography. The post-operative tractography was performed by aligning all subjects' FA maps into common standard space (MNI template) using SPM normalization. The post-operative FA maps were co-registered into preoperative FA maps and created ROI masks and saved as seed points for fiber tractography. Affine registration between and pre and postoperative images accounts for distortions and brain shifts. So a non-linear registration was done, which corrected for small displacements. The measurements were performed independently by two persons blinded to the clinical data and experienced in tractography (JSJ and AR).

Statistical analysis

All statistical analysis were performed using SPSS 17 version (SPSS, Inc., Chicago, IL, USA). ANOVA test was done to compare and validate the results obtained, a p value < 0.01 was considered to be statistically significant.

Results

There were no significant differences in the mean age or gender between the controls and the patients (Table 1).

Table 1 Demographic data and tract based statistics of Meyer's loop.

	Age	Handedness	Voxel count (mean)		Tract volume (ml)		FA		MD	
			Right	Left	Right	Left	Right	Left	Right	Left
Controls (n = 75) Male = 45 Female = 30	22—37 years	Right	456	497	7.65	9.65	0.656	0.712	1202.36	986.25
Patients (n = 25) RTLE = 14 LTLE = 11	25—40 years	Right	446 485	459 467	6.36 8.24	7.25 6.86	0.565 0.899	0.789 0.621	1102.65 895.32	955.32 1224.45

n = number; RTLE = right temporal lobe epilepsy; LTLE = left temporal lobe epilepsy, FA = fractional anisotropy, MD = mean diffusivity.

Tractography studies indicated that the location of the tip of the Meyer's loop and anterior limit of the temporal horn was very close to each other, almost superimposed in majority and superior and lateral to it is located the temporal stem. Tract based statistics results are shown in Table 1 and the results of various distances measured are shown in Table 2.

The results of ANOVA showed that the left ML-TP distance was less than the right across both patients and controls (p = 0.01). The estimated average distance of Meyers loop from left temporal pole was found to be 37.44 ± 4.7 mm (range: 32.2—46.6 mm) and from right temporal pole was 39.08 ± 4.9 mm (range: 34.3—49.7 mm). The average distance of right temporal pole to the tip of the temporal horn was found to be 28.92 ± 2.09 mm (range: 25.9—33.3 mm) and left temporal pole to the tip of the temporal horn was 28.32 ± 2.03 mm (range: 26.4—32.8 mm). Estimated anterior extent of left Meyer's loop was calculated as 11.44 ± 3.2 mm (range: 7.8—18.4 mm) and anterior extent of right Meyer's loop was calculated as 10.44 ± 3.6 mm (range: 4—19.5 mm) (Fig. 3A and B). The average volume of the right Meyers's loop was estimated as 5.9 ml (range: 3.56—8.14 ml) and 6.3 ml (range: 4.44—8.26) for left. The FA and MD value for left Meyer's loop was found to be 0.584 (range: 0.441—0.741) and 972.34(range: 763.36—1302.14) and for right Meyer's loop, it was 0.573(range: 0.455—0.765) and 1003.76 (range: 845.65—1147.25) respectively. When the tract volume, voxel count, FA and MD were calculated, the radiations extending beyond the actual optic radiations were excluded meticulously. For probabilistic tractography, a FA threshold of 0.2 was chosen, so that spurious fiber tracts appear only in brain areas with FA lower than 0.2. The voxels outside the main tract may be represented as having lower probability and it was removed by thresholding process. Exclusion mask were applied to remove adjacent white matter connections such as inferior longitudinal fasciculus, inferior fronto occipito fasciculus and uncinate fasciculus. So the quantitative calculations of fiber tracts strictly involved the actual optic radiations.

When we compared the 14 patients with contra lateral complete superior quadrantanopia after surgery (10 right and 4 left) with that of 11 patients without VFD after surgery (7 left and 4 right), the safe upper limit of resection of temporal lobe from the left temporal pole was found to be 46.2 mm and from right temporal pole was 49.7 mm not to cause complete contralateral quadrantanopia. We also computed the maximum safe distance of left temporal pole to the tip of the temporal horn to be 32.9 mm and right temporal pole to the tip of the temporal horn as 33.7 mm which did not cause any VFD. To cite an example of a patient who underwent right ATL with no post-operative VFD since the resection margin did not encroach into the anterior extent of the Meyer's loop (Fig. 4) and in another patient where the

Table 2 Various measurements depicting extent of Meyer's loop in temporal lobe.

	Mean distance from the temporal pole to the anterior limit of Meyers loop (TP-ML), mm		Mean distance from the temporal pole to the tip of the temporal horn (TP-TH), mm		Mean distance from temporal horn to anterior limit of Meyers loop (TH-ML), mm	
	Left	Right	Left	Right	Left	Right
Controls	37.44	39.08	28.32	28.92	10.44	11.35
Patients						
LTLE	35.36	36.41	29.35	30.10	8.61	9.70
RTLE	38.33	37.21	31.35	28.55	8.52	7.61

RTLE = right temporal lobe epilepsy; LTLE = left temporal lobe epilepsy.

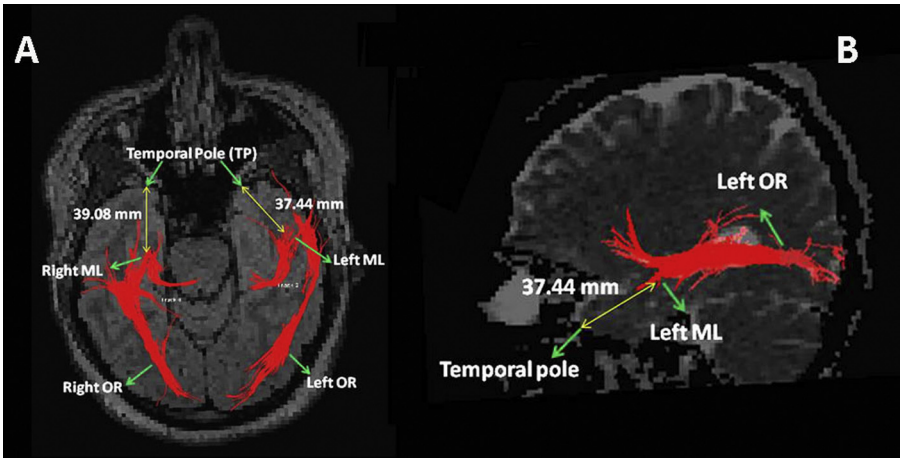

Fig. 3 (A) Axial and (B) sagittal sections showing relation of Meyers's loop (ML) to temporal pole (TP) and temporal horn (TH) and estimated average distance (TP-ML distance) of temporal pole to the anterior extent of Meyer's loop.

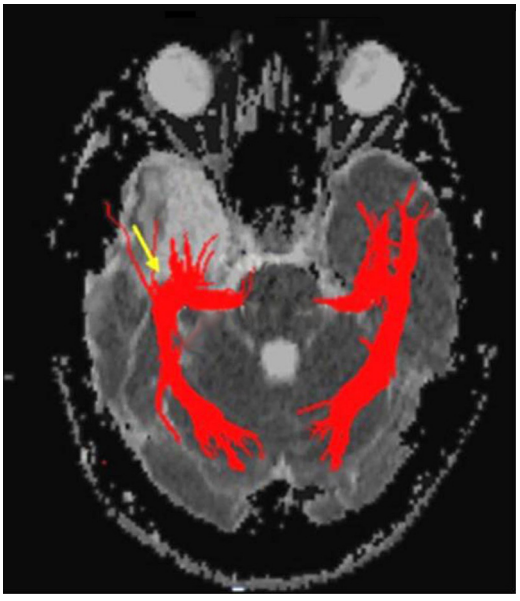

Fig. 4 A patient who underwent right anterior temporal lobectomy with no post-operative field defect since the resection margin did not encroach into the anterior extent of the Meyer's loop (arrow).

surgery inadvertently encroached the Meyer's loop causing a quadrantanopia on the opposite side is depicted in (Fig. 5A and B) respectively.

Discussion

The optic radiations (OR) are projection fibers that constitute the posterior portion of the optic pathway. They extend from the lateral geniculate nucleus (LGN) of the thalamus to the calcarine cortex. These connections traverse both the temporal and parietal lobes. They run laterally and dorsally along the temporal horn of the lateral ventricle, and laterally along the occipital horn of the lateral ventricle. The main role of OR is to convey visual information from LGN to the primary visual cortex in the occipital lobe. The fibers of the OR are divided into three bundles, inferior (ventral), superior (dorsal) and anterior (Meyer's fibers). The inferior bundle contains fibers from the inferior retina, which carry visual information from the contra lateral superior visual quadrant. Fibers carrying information from superior visual field runs anteriorly from the LGN and passes into the anterior temporal lobe before looping back to the posterior cortex. This region of the OR is called Meyer's loop (ML). The anterior part of the ML contains fibers corresponding to

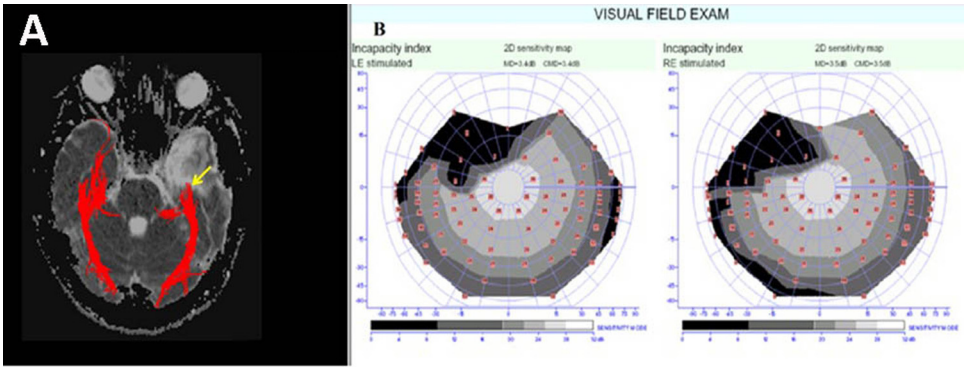

Fig. 5 (A) A patient where left anterior temporal lobectomy inadvertently encroached the Meyer's loop causing (B) right incongruous superior quadrantnopia.

the medial part of the upper quadrant, whereas in the posterior part, there are fibers that correspond to the lateral part of the upper quadrant. Because the anterior portion of the ML is more likely to be injured during a temporal lobe resection, field defects after ATL causes denser medial deficits in field than lateral and sometimes lateral sector can even be spared leading to an incomplete superior quadrantanopia. When the injury to the ML becomes total, the patient develops complete upper quadrant VFD.

VFD cannot be accurately predicted by conventional MR imaging or from the extent of the resection performed on the temporal lobe. Risk of damage to the ML may be substantial at times because the tracts are not separately visible under the operating microscope. This complication although can be considered minor as far as a major surgery like temporal lobectomy is considered, this becomes especially important for those who are employed in specific occupations like driving and whose daily life mandates driving. In many developed countries there are guidelines on VFDs, failing which they lose their driving license which causes a major impediment in their day to day lives (Medical standards, 2006). In UK, 25—46% of patients fail the current visual field criteria after ATL set by the UK Driver and Vehicle Licensing Authority, even if they are seizure free (Manji and Plant, 2000; Pathak et al., 2002). Pathak et al. (2002) from Wales found that only 50% of 14 patients post-temporal lobectomy could pass the visual examination required to drive.

Various clinical studies reported on the intersubject variability in the anterior extent of ML and the occurrence of VFD due to damage of the anterior part of the optic radiation during temporal lobe resections. The results were variable with the largest difference between studies being more than 20 mm (Jensen and Seedorff, 1976; Barton et al., 2005; Salmon et al., 2000; Nilsson et al., 2004; Marino and Rasmussen, 1968; Hughes et al., 1999; Egan et al., 2000; Powell et al., 2005; Nilsson et al., 2007; Sherbondy et al., 2008; Winston et al., 2012). The incidence of VFDs seems to be increasingly appreciated because of the increased sensitivity of automated computerized perimetry in identifying even small defects compared with static manual perimetry used earlier. The most powerful validation is by comparison of VFDs pre- and post-operatively in any individual. Unfortunately, the results even after applying VFD comparison are still quite variable (Barton et al., 2005; Nilsson et al., 2007; Chen et al., 2009). Some studies have reported that the extent of VFD is proportional to the degree of resection of the temporal lobe (Hughes et al., 1999; Winston et al., 2012), few others have refuted it (Tecoma et al., 1993). This itself underscores the fact that the extent and dimensions of ML is quite heterogeneous in different groups. Knowledge of the limits of the ML and the OR in normal population is by and large needed to accurately predict the chance of VFD in a person undergoing ATL for refractory TLE or a temporal resection for other reasons; this would be an important advantage in pre-surgical counseling. This prompted us to analyze a large cohort of normal subjects and patients (pre- and post-ATL) with DTIT aided mapping of ML to assess their VFDs.

We assessed the overall antero-posterior extent of OR using fiber tracking probabilistic algorithm. This is more superior to the deterministic models where the crossing and kissing fibers interferes and therefore one can underestimate the real anterior extent of the ML. We found that there is extensive inter individual variability in the degree of the anterior extent of the ML. In most of the normal subjects (78%), left Meyer's loop extended more anteriorly than right (mean 7.4 ± 0.8 mm). This is in line with the observations of previous studies (Yogarajah et al., 2009; Jeelani et al., 2010; Wang et al., 2010). Yogarajah et al. (2009) combined retrospective probabilistic fiber tracking in 20 controls and 21 postsurgical patients with postoperative assessment of VFDs using Goldmann perimetry. Nine of 21 patients had VFDs and a distance of <35 mm from the tip of the Meyer's loop to the TP was considered as detrimental in causing VFDs. In a recent study by Winston et al. (2012), on 20 patients undergoing anterior temporal resections, tractography of the optic radiations was done pre-operatively and propagated to post-operative images. They noted that Meyer's loop was 4.4—18.7 mm anterior to the resection margin in patients with VFD, but 0.0—17.6 mm behind the resection margin in eight patients without VFD. Another study showed left-sided resections as causing significantly high risk of VFDs as compared to right sided resections as in our population (Jeelani et al., 2010). Also, the difference in the distance from temporal horn to the anterior limit of Meyer's loop (TH-ML) was also quite variable, with distances varying over 19 mm on an average. We found that the upper limit of ML-TP distance was 35.4 mm on the left side and 38.1 mm on the right side in normal subjects.

After optimizing the results, we tried to track the post-surgical tractography of ML in post ATL patients with the same seed points and other parameters to demonstrate the extent of resection and VFD. On analysis of the patients in comparison to the controls, we found that if the anterior limit of the ML was $\leq$38 mm on the right and $\leq$35 mm on the left from the temporal pole, they are at a greater risk of developing VFDs. We propose that a ML-TP distance of 35 mm on the left and 38 mm on the right can thus be considered as a safe limit for resection of the temporal lobe in refractory TLE where the fields will be totally intact. The commuted safe upper limit of resection of temporal

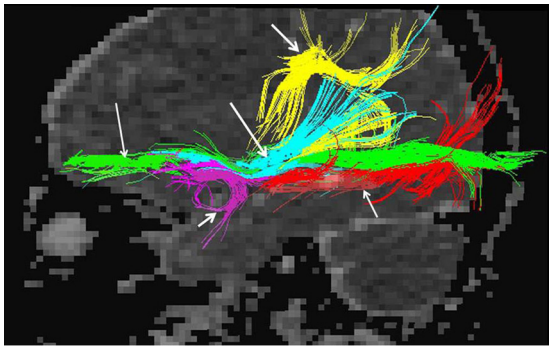

Fig. 6 Tractography of various language related fiber tracts showing close relationship to the Meyer's loop fibers (short thin arrow) (red). Inferior fronto-occipital fasciculus (long thin arrow) (green), inferior longitudinal fasciculus (long thick arrow) (blue), superior longitudinal fasciculus (medium thick arrow) (yellow) and uncinate fasciculus (short thick arrow) (pink). (For interpretation of the references to color in this figure legend, the reader is referred to the web version of this article.)

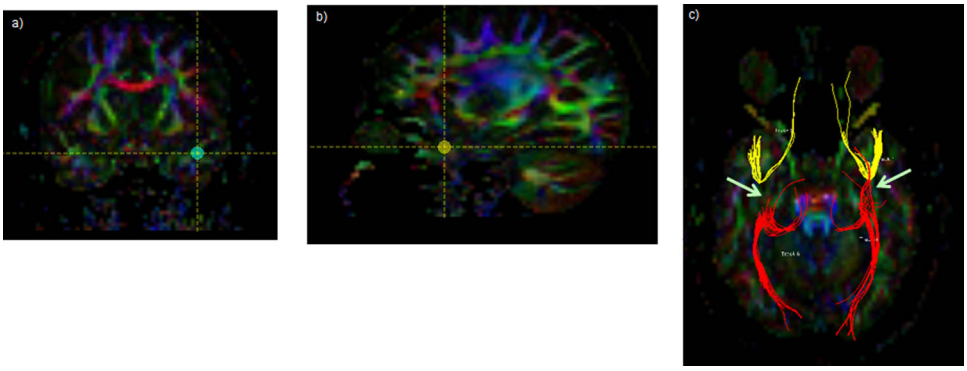

Fig. 7 Tractography of uncinate fasciculus (UF) and its relation to Meyer's loop (ML). For UF tarctography, (a) first seed region was drawn on the posterior aspect of lateral orbito-frontal region in coronal plane (blue) and (b) second seed region (yellow) was drawn on the antero-inferior temporal lobe area in sagittal plane. (c) UF and ML tracts were superimposed on FA map, note that UF lies anterior to the ML. (For interpretation of the references to color in this figure legend, the reader is referred to the web version of this article.)

lobe from the left temporal pole was found to be 46.2 mm and from right temporal pole was 49.7 mm, beyond which a complete contra lateral quadrantanopia occurs which causes problems in daily life and driving in most cases unlike incomplete, minor defects. We have tried to outline the various series existing in literature depicting the anatomy of ML by DTIT and have compared their results with ours (Supplementary Table S1).

Supplementary Table S1 related to this article can be found, in the online version, at http://dx.doi.org/10.1016/j.eplepsyres.2014.11.020.

Tractographic analysis of OR also showed a close relationship with language related fiber tracts such as inferior fronto-occipital fasciculus, inferior longitudinal fasciculus and inferior aspect of superior longitudinal fasciculus (parieto-occipito-temporo-pontine fasciculi) and uncinate fasciculus (Fig. 6). By tracking these adjoining tracts, we tried to minimize the error of under-visualization of white matter tracts by DTIT which is an inherent error in this tracking procedure (Kinoshita et al., 2005). These tracts are in close proximity crossing one another, forming the sagittal stratum in the occipital lobe. Kier et al. (2004) reported that the posterior limit of the uncinate fascicles and the anterior limit of the Meyer loop meet closely, like kissing, within the temporal stem, by a post-mortem MR imaging study with dissection (Kier et al., 2004). The visual pathways can be differentiated from them, as only ORs run through LGN (Fig. 6). The uncinate fasciculus lies just anterior to the tip of the Meyer's loop and can be also used for placing a seed point for tracking the Meyer's loop (Fig. 7).

Merits and limitations

Our study deserves merit in that it included a large sample size of both patients and controls. A uniform surgical technique (none underwent selective amygdalo-hippocampectomy) was used thus overcoming clinical heterogeneity. Pre- and post-operative automated perimetry was done homogeneously in patients to accurately assess VFD unlike in other studies. By using probabilistic algorithm, the difficulty of tracking kissing and crossing fibers in ML was overcome which could have under-estimated the anterior extent of ML. By tracking adjoining tracts, especially uncinate fasciculus, we further tried to minimize the error of under-visualization of white matter tracts by DTIT. It therefore lended land marks and measurements to go for pre-surgical risk assessment in ATL.

We accept the following shortcomings of our study. Tracking algorithms and technique limitations may fail to demonstrate oblique or parallel fiber tracts or tracts with large and/or sharp curvature. The inferior longitudinal and parieto-occipito-temporo-pontine fascicles are very close to each other, potentially affecting the assessment of the location and size of the OR in DTI tractography studies (Miller, 2005). Another important limitation of DTIT is lack of sufficient spatial resolution which leads to increased chances of occurrence of false positive fibers (Hofer et al., 2010). The study by Staempfli et al. demonstrated that visual pathway tracking with the help of a fast marching tracking algorithm is prone to generate a large number of false positive fibers (Staempfli et al., 2008). But we used 2 mm isotropic voxels which gives a better resolution and is superior for the identification of fiber tracts. To establish the reproducibility of the study and for the easy assessment of fiber statistics, we used multiple ROI technique with same radius and the two ROIs were placed correctly in the respective brain regions, so tracking excludes all fiber tracks that do not directly connect both regions. The selection of FA threshold is also an important factor to be considered during tract reconstruction. High FA values results in generation of fewer fibers, whereas lower FA values generate more fibers. We used the FA threshold value of 0.2. Our results could have been better with a 3 T MRI instead of 1.5 T, which has been shown to provide a better estimate of the DTIT by improving the resolution and signal-to-noise ratio (Chen et al., 2009; Alexander et al., 2002).

Conclusion

DTIT can be considered as a novel and relatively easy technique to delineate OR and ML and to study the anatomic variability between individuals. It also plays an important

role in planning surgical resection of the temporal lobes and to predict an individual patient's post-operative visual performance and disability. Prospective, blinded studies using DTIT with different resection sizes assessing the extent of ML in large samples may be ideal in deriving at more robust conclusions since most of the studies including ours are retrospective in nature. However, such an endeavor may be ethically unreasonable since the extent of resection of temporal lobe needed to make the patient seizure-free may be in conflict with the amount of tissue needed to be preserved to cause no VFD. So a real time neuronavigation system incorporating DTIT of ML and intra-operative MRI may be selectively utilized to preserve visual fields in whom it is warranted. In others, with the existing data on the extent of ML as we derived in a specific population, one can effectively counsel the patients pre-operatively.

Ethical approval

We confirm that we have read the Journal's position on issues involved in ethical publication and affirm that this report is consistent with those guidelines.

Conflict of interest

None of the authors has any conflict of interest to disclose nor any funding is taken from any individual or organization.

Acknowledgments

We thank Mr. Jigish B. Modi, Modi Medicare for providing Myrian XT-Brain (Intrasense-Modi Medicare). We also acknowledge all the present and past staff and faculty of our center who indirectly helped us in many ways to complete this study.

References

Alexander, D.C., Barker, G.J., Arridge, S.R., 2002. Detection and modeling of non-Gaussian apparent diffusion coefficient profiles in human brain data. Magn. Reson. Med. 48, 331—340.

Barton, J.J., Hefter, R., Chang, B., Schomer, D., Drislane, F., 2005. The field defects of anterior temporal lobectomy: a quantitative reassessment of Meyer's loop. Brain 128, 2123—2133.

Basser, P.J., 1995. Inferring microstructural features and the physiological state of tissues from diffusion-weighted images. NMR Biomed. 8, 333—344.

Chen, X., Weigel, D., Ganslandt, O., Buchfelder, M., Nimsky, C., 2009. Prediction of visual field deficits by diffusion tensor imaging in temporal lobe epilepsy surgery. NeuroImage 45, 286—297.

Ebeling, U., Reulen, H.J., 1988. Neurosurgical topography of the optic radiation in the temporal lobe. Acta Neurochir. (Wien) 92, 29—36.

Egan, R.A., Shults, W., So, T., Burchiel, N., Kellogg, K.J., Salinsky, X.M., 2000. Visual field deficits in conventional anterior temporal lobectomy versus amygdalohippocampectomy. Neurology 55, 1818—1822.

Hofer, S., Karaus, A., Frahm, J., 2010. Reconstruction and dissection of the entire human visual pathway using diffusion tensor MRI. Front. Neuroanat. 13 (4), 15.

Hughes, T.S., Abou, K.B., Lavin, P.J., Fakhoury, T., Blumenkopf, B., Donahue, S.P., 1999. Visual field defects after temporal lobe resection: a prospective quantitative analysis. Neurology 53, 167—172.

Jeelani, N.U., Jindahra, P., Tamber, M.S., Poon, T.L., Kabasele, P., James-Galton, M., Stevens, J., Duncan, J., McEvoy, A.W., Harkness, W., Plant, G.T., 2010. Hemispherical asymmetry in the Meyer's loop: a prospective study of visual-field deficits in 105 cases undergoing anterior temporal lobe resection for epilepsy. J. Neurol. Neurosurg. Psychiatry 81, 985—991.

Jensen, I., Seedorff, H.H., 1976. Temporal lobe epilepsy and neuro-ophthalmology. Ophthalmological findings in 74 temporal lobe resected patients. Acta Ophthalmol. 54, 827—841.

Kier, E.L., Staib, L.H., Davis, L.M., Bronen, R.A., 2004. MR imaging of the temporal stem: anatomic dissection tractography of the uncinate fasciculus, inferior occipitofrontal fasciculus, and Meyer's loop of the optic radiation. Am. J. Neuroradiol. 25, 677—691.

Kinoshita, M., Yamada, K., Hashimoto, N., Kato, A., Izumoto, S., Baba, T., Maruno, M., Nishimura, T., Yoshimine, T., 2005. Fiber-tracking does not accurately estimate size of fiber bundle in pathological condition: initial neurosurgical experience using neuronavigation and subcortical white matter stimulation. NeuroImage 25, 424—429.

Salmon, K., Guenot, P.M., Tiliket, C., Isnard, J., Sindou, M., Mauguiere, F., Vighetto, A., 2000. Anatomy of optic nerve radiations as assessed by static perimetry and MRI after tailored temporal lobectomy. Br. J. Ophthalmol. 84, 884—889.

Manji, H., Plant, G.T., 2000. Epilepsy surgery. Visual fields, and driving: a study of the visual field criteria for driving in patients after temporal lobe epilepsy surgery with a comparison of Goldmann and Esterman perimetry. J. Neurol. Neurosurg. Psychiatry 68, 80—82.

Marino Jr., R., Rasmussen, T., 1968. Visual field changes after temporal lobectomy in man. Neurology 18, 825—835.

2006. Medical standards for licensing and clinical management guidelines: section 23 vision and eye disorders — assessing fitness to drive. Austroads Inc, 23.2.3 and 23.3.1:96-10.

Miller, N.R., 2005. Diffusion tensor imaging of the visual sensory pathway: are we there yet? Am. J. Ophthalmol. 140, 896—897.

Mori, S., Van, Z.P.C., 2002. Fiber tracking: principles and strategies — a technical review. NMR Biomed. 15, 468—480.

Nilsson, D., Malmgren, V., Rydenhag, B., Frisén, L., 2004. Visual field defects after temporal lobectomy — comparing methods and analysing resection size. Acta Neurol. Scand. 110, 301—307.

Nilsson, D., Starck, G., Ljungberg, M., Ribbelin, S., Jönsson, L., Malmgren, K., Rydenhag, B., 2007. Intersubject variability in the anterior extent of the optic radiation assessed by tractography. Epilepsy Res. 77, 11—16.

Pathak, R.V., Ray, V., Walters, R., Hatfield, R., 2002. Detection of visual field defects in patients after anterior temporal lobectomy for mesial temporal sclerosis-establishing eligibility to drive. Eye (Lond.) 16, 744—748.

Powell, H.W.R., Parker, G.J.M., Alexander, D.C., Symms, M.R., Boulby, P.A., Wheeler, K.C.A., Barker, G.J., Koepp, M.J., Duncan, J.S., 2005. MR tractography predicts visual field defects following temporal lobe resection. Neurology 65, 596—599.

Radhakrishnan, A., James, J.S., Kesavadas, C., Thomas, B., Bahuleyan, B., Abraham, M., Radhakrishnan, K., 2011. Utility of diffusion tensor imaging tractography in decision making for extratemporal resective epilepsy surgery. Epilepsy Res. 97, 52—63.

Sherbondy, A.J., Dougherty, R.F., Napel, S., Wandell, B.A., 2008. Identifying the human optic radiation using diffusion imaging and fiber tractography. J. Vis. 12, 1—11.

Staempfli, P., Reischauer, C., Jaermann, T., Valavanis, A., Kollias, S., Boesiger, P., 2008. Combining fMRI and DTI: a framework for exploring the limits of fMRI-guided DTI fiber tracking and for verifying DTI-based fiber tractography results. NeuroImage 39, 119—126.

Taoka, T., Sakamoto, M., Nakagawa, H., Nakase, H., Iwasaki, S., Takayama, K., Taoka, K., Hoshida, T., Sakaki, T., Kichikawa, K., 2008. Diffusion tensor tractography of the Meyer loop in cases of temporal lobe resection for temporal lobe epilepsy: correlation between postsurgical visual field defect and anterior limit of Meyer loop on tractography. Am. J. Neuroradiol. 29, 1329—1334.

Taoka, T., Sakamoto, M., Iwasaki, S., Nakagawa, H., Fukusumi, A., Hirohashi, S., Taoka, K., Kichikawa, K., Hoshida, T., Sakaki, T., 2005. Diffusion tensor imaging in cases with visual field defect after anterior temporal lobectomy. Am. J. Neuroradiol. 26, 797—803.

Tecoma, E.S., Laxer, K.D., Barbaro, N.M., Plant, G.T., 1993. Frequency and characteristics of visual field deficits after surgery for mesial temporal sclerosis. Neurology 43, 1235—1238.

Wang, Y.X., Zhu, X.L., Deng, M., Siu, D.Y., Leung, J.C., Chan, Q., Chan, D.T., Mak, C.H., Poon, W.S., 2010. The use of diffusion tensor tractography to measure the distance between the anterior tip of the Meyer loop and the temporal pole in a cohort from Southern China. J. Neurosurg. 113, 1144—1151.

Winston, G.P., Daga, P., Stretton, J., Modat, M., Symms, M.R., McEvoy, A.W., Ourselin, S., Duncan, J.S., 2012. Optic radiation tractography and vision in anterior temporal lobe resection. Ann. Neurol. 71, 334—341.

Yogarajah, M., Focke, N.K., Bonelli, S., Cercignani, M., Acheson, J., Parker, G.J., Alexander, D.C., McEvoy, A.W., Symms, M.R., Koepp, M.J., Duncan, J.S., 2009. Defining Meyer's loop-temporal lobe resections, visual field deficits and diffusion tensor tractography. Brain 132, 1656—1668.